splitting, could well lead to lack of any ESR transitions (at least at X-band frequency).

Assuming that the magnitude of zero-field splitting terms, which originate in the kinds of interactions shown in Table VI, determines the observance or nonobservance of lines, we are left with the intriguing question of what factors in the enzyme lead to ESR silence. One possibility is a difference in the Fe–Cu distances and/or bridging mode of the CN^- group. Another possibility is the differences in g-term anisotropies (and hence ligand-field symmetries) on the Cu and Fe centers in the cyano enzyme compared to our model system, influenced by structural or other features of the protein matrix. As noted earlier in the solution behavior section, it is possible to simulate such effects in a crude way in the ESR tube by using DMF as solvent for the $[Fe(P)CNCu(N_4)]^{2+}$ complex. On the other hand, solutions in $CHCl_3$–MeOH with or without added 1-methylimidazole exhibit ferromagnetic coupling and an ESR triplet spectrum, whereas MeCN or Me_2SO solutions show little or no coupling. Further elucidation of these subtle but important features may be solved by low-temperature solution magnetic susceptibility, MCD, magnetization, and Mössbauer measurements or ultimately by X-ray crystallographic studies.

Acknowledgment. We thank Paul E. Clark and Mark Irving for the Mössbauer spectra and John Pilbrow for discussions on ESR spectroscopy. Discussions with Andrew Thomson on some aspects of this work are also gratefully acknowledged. K.S.M. acknowledges support from the Australian Research Grants Scheme and the Monash University Special Research Fund.

Registry No. 1, 90148-73-5; $Fe(P)Cl(N_4)$, 90242-08-3; $Fe(P)\overline{CN(N_4)}$, 90148-74-6; $H_2O\overline{FeCNCu}(H_2O)$, 90148-76-8; $MeOH\overline{FeCNCu}(MeOH)$, 90148-78-0; $MeIM\overline{FeCNCu}(MeOH)$, 90148-80-4; $NC\overline{Fe}\overline{MeCN}\ \overline{CuMeCN}$, 90148-82-6; $NC\overline{FeMe_2SO}\ \overline{CuMe_2SO}$, 90148-84-8; $DMF\overline{FeCNCu}DMF$, 90148-86-0; $Fe(P)OH(N_4)$, 90242-09-4.

Supplementary Material Available: Table listing χ_M, μ_{eff} (μ_B), and temperature (K) data for compound **1** (1 page). Ordering information is given on any current masthead page.

Systematic Trends in Metalloporphyrin Optical Spectra

M.-Y. Rachel Wang[1] and Brian M. Hoffman*[2]

Contribution from the Department of Chemistry, Northwestern University, Evanston, Illinois 60201, and the Department of Chemistry, Whitworth College, Spokane, Washington 99251. *Received September 29, 1983*

Abstract: We report the effects of axial ligands (L) on the optical spectra of cobalt-substituted myoglobin, horseradish peroxidase, and cytochrome $P450_{cam}$. In addition, we present data for a series of octapyrrole-substituted zinc porphyrin complexes. The response of a metalloporphyrin to the change of ligand is more complicated than previously noted and is not the same for pyrrole-substituted porphyrins as it is for meso-tetraaryl-substituted compounds. Perturbations by the ligand not only shift the overall spectrum as previously observed but also systematically change the frequency difference between the Soret (B) and the α–β (Q) bands. The observed trends in band frequencies can nevertheless be readily understood within the four-orbital model of Gouterman. Interpretation of band intensities is less clear.

Metal-substituted hemoproteins provide an ideal system for studies of metalloporphyrin properties,[3] and in this paper we report the effects of axial ligands (L) on the optical spectra of cobalt-substituted myoglobin, horseradish peroxidase, and cytochrome $P450_{cam}$. In addition, we present optical data for a series of octasubstituted zinc porphyrins, namely, zinc meso-, octaethyl-, and protoporphyrin complexes; since zinc porphyrins bind only a single axial ligand, they also provide a convenient system for systematically studying the influences of axial ligation. Cobalt and zinc porphyrins each exhibit only a single spin state (Co ($S = {}^1/_2$); Zn ($S = 0$)),[4] so complications from spin changes are absent.

The general pattern of a normal metalloporphyrin spectra is well-known.[4] It typically exhibits two moderately intense bands, the so-called α–β bands ($\epsilon \cong 10^4\ M^{-1}\ cm^{-1}$), in the vicinity of ~550 nm and an extremely strong band, the Soret, in the vicinity of ~400 nm ($\epsilon \sim 10^5\ M^{-1}\ cm^{-1}$) see Figure 1). In first approximation, these bands can be considered as π–π^* excitations localized on the porphinato macrocycle, and the overall nature of the spectra can be explained by reference to Gouterman's "four-orbital" mode[5,6,7] shown in Figure 2. This model focuses on transitions from the two highest occupied porphyrin π-molecular orbitals (a_{2u} and a_{1u} in D_{4h} symmetry) into the lowest pair of unoccupied MO's (e.g., in D_{4h} symmetry). The $a_1 \rightarrow e$ and $a_2 \rightarrow e$ excitations give rise to four excited configurations which are equivalent in pairs. They undergo pairwise configuration interaction to give the excited state that correspond to the Soret, or B, band, and the α–β, or Q, excitations. These excited configurations and resulting configuration mixed states are shown in Figure 2B.

The need for a detailed understanding of porphyrin spectra has led to the systematic correlation of spectra from complexes with different metals, peripheral substituents, and axial ligands.[4,8–12] These studies have shown that the α–β and Soret bands undergo frequency shifts in response to variations in metal and/or axial base and that the shifts correlate with variations in extinction

(1) Department of Chemistry, Whitworth College, Spokane, WA 99251.
(2) Northwestern University.
(3) Hoffman, B. M. In "The Porphyrins"; Dolphin, D., Ed., Academic Press: New York, 1978; Vol. III.
(4) Gouterman, M. In "The Porphyrins"; Dolphin, D., Ed.; Academic Press: New York, 1978; Vol. III.
(5) Gouterman, M. *J. Mol. Spectrosc.* **1961**, *6*, 138–163.
(6) Gouterman, M.; Wagniere, G. H.; Snyder, L. C. *J. Mol. Spectrosc.* **1963**, *11*, 108–127.
(7) Spellane, P. J.; Gouterman, M.; Antipas, A.; Kim, S.; Liu, Y. C. *Inorg. Chem.* **1980**, *19*, 386.
(8) Gouterman, M. *J. Chem. Phys.* **1959**, *30*, 1139–1161.
(9) Zerner, M.; Gouterman, M. *Theor. Chim. Acta* **1960**, *4*, 44–63.
(10) Antipas, Y. A. Ph.D. Thesis, University of Washington, Seattle, WA, 1979.
(11) Nappa, M.; Valentine, J. S. *J. Am. Chem. Soc.* **1978**, *100*, 5075–5080.
(12) Gouterman, M.; Schwartz, F.; Smith, P. D.; Dolphin, D. *J. Chem. Phys.* **1973**, *59*, 676.

0002-7863/84/1506-4235$01.50/0

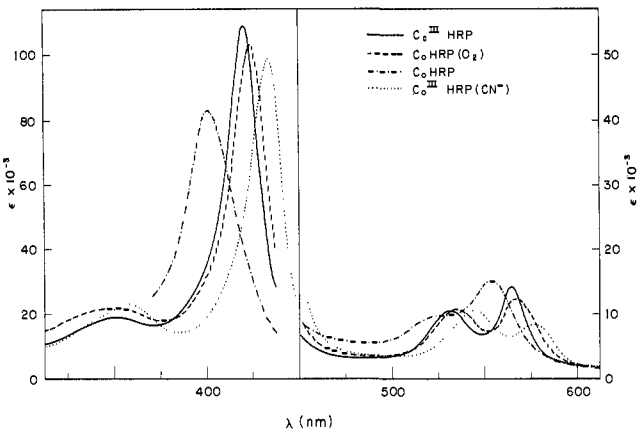

Figure 1. Optical absorption spectra of cobalt-substituted HRP (B, C isozymes; pH 8.2, 0.05 M Tris HCl).

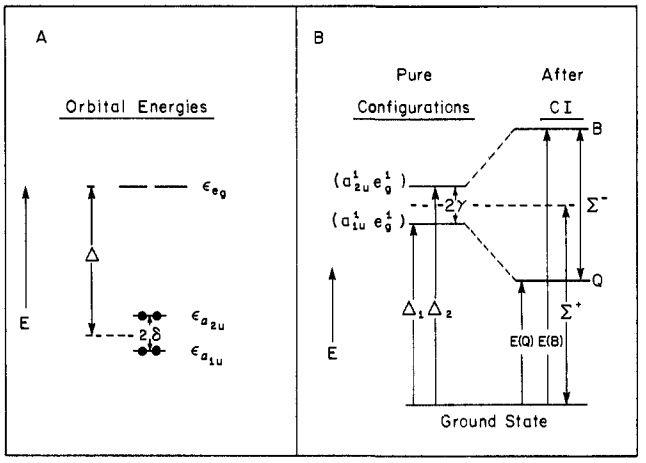

Figure 2. Typical π-electron energy level scheme for a closed-shell metalloporphyrin: (A) one-electgron energies of highest occupied and lowest unoccupied π-molecular orbitals; (B) configuration energies for the lowest π-excitations before (left) and after right) configuration interaction. Symbols are defined in text; in particular, see Discussion.

coefficients, for example in the ratio $\epsilon_\alpha/\epsilon_\beta$. Gouterman[8] found that the electronegativity of a metal ion correlated surprisingly well with the absorption band energies and extinction ratios, and Nappa and Valentine[11] explained their results for the Zn(TPP)(L)[13] in an analogous fashion, concluding that the charge and polarizability of L, not the Zn–L bond strength, control the red shift. Such correlations have also been rationalized within the four-orbital model. For example, changes in metal and/or axial ligand are considered to cause a shift in the B and Q bands largely because interactions with the metal influence the one-electron energy of the a_{2u} orbital.[8,11,12] The a_{1u} orbital has nodes at the pyrrole nitrogen and so should be much less influenced by perturbations of the central metal.[6]

Our observations confirm that varying the axial ligand of a given metalloporphyrin indeed causes appreciable overall shifts in the porphyrin visible spectrum, the shifts being best measured as the average configuration energy (Σ^+, Figure 2). However, we also find that the response of a metalloporphyrin to the change of ligand is more complicated than previously indicated and is not the same for pyrrole-substituted porphyrins as it is for the meso-tetraaryl-substituted compounds.[14] This report presents the first observations which clearly show that perturbations by the ligand also systematically change the frequency difference between the Soret (B) and the α–β (q) bands (Σ^-, Figure 2). The trends in band frequencies can still be readily understood within the four-orbital model. However, the trends in the relative band intensities, as measured by ratios of extinction coefficients, do not appear to follow readily from the simpest form of the model.

Experimental Procedures

Protoporphyrin IX was prepared from hemin chloride by a modified ferrous sulfate method[14,15] and proved to be pure by thin-layer chromatography on Eastman Kodak silica gel plates in a 70:30:15:10:2 (v/v) benzene–ethyl formate–formic acid–dioxane–water solvent system. Cobalt protoporphyrin IX was prepared by a modification of the method of Yonetani et al.[16] The metalloporphyrin showed only one spot at R_f 0.68 by TLC tests on silica gel plates with a 50:1.5:1.4 (v/v) butanol–acetic acid–H_2O solvent system and gave the α–β peak intensity ratio $\epsilon_\alpha/\epsilon_\beta$ = 1.04 in 1:10 (v/v) pyridine–0.1 N NaOH.

The general procedures for preparing metal-substituted hemoproteins have been described.[17] Lyophilized, salt free myoglobin (Mb) and horseradish peroxidase (HRP) were obtained from Sigma Chemical Co. The peroxidase was further purified by the method described by Shannon et al.[18] Two isozyme fractions were used, i.e., HRP(A) and HRP(B, C), according to the classification of Paul[19] and Shannon et al.[18] Cobalt-substituted myoglobin (Co^{II}(Mb))[20] and horseradish peroxidases (Co^{III}(HRP))[21] were prepared as described. The cobaltic myoglobin was prepared by oxidizing a solution of Co^{II}Mb (pH 8.2, Tris buffer, 0.05 M) at 0 °C with ferricyanide for 30 min, followed by deionization on a mixed-bed ion exchange column (Rexyn I-300, H–OH form) and dialysis into appropriate buffers for further studies. Cytochrome $P450_{cam}$ was isolated and purified from *Pseudomonas putida* PpG786 (AT CC 29607) grown on D-(+)-camphor as the sole carbon and energy substrate.[22] The cobalt-substituted protein was prepared as described earlier.[15,23]

Zinc mesoporphyrin IX dimethyl ester (Zn(mesoDME)) and zinc octaethylporphyrin (Zn(OEP)) were prepared from the parent porphyrins (Sigma and Aldrich, respectively) and zinc acetate by the method of Adler et al.[24] Both Zn(OEP) and Zn((meso)DME) were recrystallized from toluene under a dry N_2 atmosphere and heated under vacuum at 90 °C to remove H_2O. Toluene was distilled from Na and stored over Molecular Sieves (Linde, 4A). Imidazole was recrystallized from benzene under N_2. Methylimidazole was vacuum distilled. Other reagents were used as received.

Optical spectra were taken with 1 cm path length cuvettes on a Beckman Acta III spectrophotometer at room temperature. The protein solutions were generally ~2 μM protein in either 0.05 M Tris buffer (pH 7.5–9) or potassium phosphate buffer (pH 6–8). Specific conditions are given in Table I.

Results

Figure 1 presents the optical spectra of several forms of cobalt-substituted horseradish peroxidase.[21] One can readily see that Soret and α–β bands shift upon variation in the oxidation

(13) Abbreviations used here to denote the various metalloporphyrins and metal-substituted hemoproteins follow the nomenclature system of ref 4 and 18. As a typical example, Co^{II}(proto)(Im) specifies the central metal ion Co in 2+ charge state with protoporphyrin IX (i.e., proto), as the porphyrinato ring system and an axial ligand imidazole (Im). Other porphyrins used: ((meso)DME) mesoporphyrin IX dimethyl ester; (OEP) octaethylporphyrin; (TPP) tetraphenylporphyrin; ((proto)DME) protoporphyrin IX dimethyl ester. Ligands are abbreviated as follows: 18C6, 18-crown-6 ether; Im^-, imidazolate; py, pyridine; pip, piperidine; SBu^-, 1-butene thiolate; His, histidine; NMeIm, *N*-methylimidazole; DTE, dithioerythritol. Unless otherwise noted, the porphyrin used in metal-substituted hemoproteins is protoporphyrin IX. Abbreviations used for the protein moieties: Hb, hemoglobin; Mb, myoglobin; HRP, horseradish peroxidase; CCP; cytochrome *c* peroxidase; Cytc, cytochrome *c*; $P450_{cam}$, cytochrome *c* P450 camphor; P420, the denatured forms of $P450_{cam}$.

(14) Wang, M.-Y. R. Ph.D. Thesis, Northwestern University, Evanston, IL, 1979.
(15) Fuhrhop, J.-H.; Smith, K. M., Eds., "Laboratory Methods in Porphyrins and Metalloporphyrins Research"; Elsevier Science Publishing: Amsterdam, 1975.
(16) Yonetani, T.; Yamamoto, H.; Woodrow, G. V., III *J. Biol. Chem.* **1974**, *249*, 682–690.
(17) Scholler, D. M.; Wang, M. R.; Hoffman, B. M. *Methods Enzymol.*, **1978**, *52*.
(18) Shannon, L. M.; Kay, E.; Lin, J. Y. *J. Biol. Chem.* **1966**, *241*, 2166–2172.
(19) Paul, K. G. *Acta Chem. Scand.* **1958**, *12*, 1312–1318.
(20) Hoffman, B. M.; Spilburg, C. A.; Petering, D. M. *Cold Spring Harbor Symp. Quant. Biol. 36*, 343–348.
(21) Wang, M.-Y. R.; Hoffman, B. M.; Hollenberg, P. F. *J. Biol. Chem.* **1977**, *252*, 6268–6275.
(22) Wagner, G. C.; Gunsalus, I. C. *Methods Enzymol.* **1978**, *52*, 1660.
(23) Wagner, G.; Gunsalus, I. C.; Wang, M.-Y. R.; Hoffman, B. M. *J. Biol. Chem.* **1981**, *256*, 6266–6273.
(24) Adler, A. D. *J. Inorg. Nucl. Chem.* **1970**, *32*, 2443–2445.

Table I. Electronic Absorption Spectra of Cobalt-Substituted Hemoproteins

	Soret		β		α			
complex[a]	nm	$cm^{-1} \times 10^3$	nm	$cm^{-1} \times 10^3$	nm	$cm^{-1} \times 10^3$	$\epsilon_\alpha/\epsilon_\beta$	$\epsilon_\alpha/\epsilon_B$
Co^{II}(Mb)	405	24.7	(520)	(19.2)	555	18.0	~1.3	
Co^{III}(Mb)(H_2O)	424	23.6	535	18.7	572	17.5	0.95	0.17
Co^{III}(Mb)(O_2)	424	23.6	537	18.6	575	17.4	1.01	0.10
Co^{III}(Mb)(His)	426	23.5	533	18.8	570	17.5	0.85	
Co^{III}(Mb)(MeIm)	427	23.4	540	18.5	575	17.4	0.78	
Co^{III}(Mb)(OH^-)	428	23.4	542	18.4	577	17.3	0.80	
Co^{III}(Mb)(N_3^-)	431	23.2	540	18.5	575	17.4	0.78	
Co^{II}(Hb)[b]	402	24.9	(523)	(19.1)	552	18.1	~1.7	0.15
Co^{III}(Hb)(O_2^-)[b]	422	23.7	538	18.6	571	17.5	1.00	0.12
Co^{III}(Hb)(CN^-)[b]	435	23.0						
Co^{II}(HRP)	401	24.9	(520)	(19.2)	553	18.1	~1.6	0.18
Co^{III}(HRP)(DTE)[c]	420	23.8						
Co^{III}(HRP)(H_2O)	421	23.8	533	18.8	565	17.7	1.45	0.13
Co^{III}(HRP)(F^-)	423	23.6	535	18.7	567	17.6	1.16	0.10
Co^{III}(HRP)(O_2^-)	424	23.6	535	18.7	567	17.6	1.15	0.12
Co^{II}(HRP)(NO)	426	23.5	540	18.5	572	18.5	1.09	
Co^{III}(HRP)(His)	426	23.5	537	18.6	572	17.5	1.01	
Co^{III}(HRP)(OH^-)	427	23.4	538	18.6	572	17.5	0.95	0.085
Co^{III}(HRP)(N_3^-)	430	23.3	540	18.5	570	17.5	0.94	0.091
Co^{III}(HRP)(CN^-)	436	22.9	545	18.4	577	17.3	0.80	0.086
$Co^{III}(P450_{cam})(H_2O)$[d]	398	25.1	515	19.4	557	18.0	2.75	0.30
Co^{II}(P450)	405	24.7						
$Co^{II}(P450_{cam})$	412	24.3	525	19.0	555	18.0	~1.9	0.22
Co^{III}(P450)(H_2O)[d]	423	23.6	535	18.7	569	17.6	1.06	0.15
$Co^{III}(P450_{cam})$(aniline)	430	23.3	545	18.4	577	17.3	0.82	0.11
$Co^{III}(P450_{cam})(OH^{-1})$[d]	435	23.0	548	18.2	580			
Co^{III}(P450)(OH^-)[d]	435	23.0	548	18.2	580	17.2	0.73	
Co^{III}(P420)	435	23.0	547	18.3	580	17.2	0.71	
$Co^{III}(P450_{cam})(CN^-)$	(367) 457	21.9	568	17.6			0	0
$Co^{III}(P450_{cam})$(DTE)	(376) 467	21.4	575	17.4			0	0
Co^{II}(Cytc)[e]	416.5	24.0	520	19.2	549	18.2	1.26	
Co^{III}(Cytc)[e]	426	23.5	530	18.9	567	17.6	0175	

[a] For an individual protein the entries are ordered by increasing red shift. The protein solutions for the Mb, Hb, and HRP systems were in pH 8.2, Tris buffer, 0.05 M; the buffer used for the P450 system was pH 7, potassium phosphate, 0.05 M, and 1 mM camphor when present, unless otherwise specied. A ligand "His" is denoted for the denatured forms of cobaltic Mb and HRP (see ref 14). [b] The spectra of Co-substituted hemoglobin derivatives are taken in pH 6.65, Bis-Tris buffer, 0.05 M. The cyanide complex spectrum was not good enough for the identification of α–β bands (concentration of CN^- = 0.02 M). [c] When 2 mM DTE was added to a solution of 5 μM HRP in pH 8.2, Tris buffer, 0.05 M, slow reduction took place along with the formation of a species absorbing at ~420 nm; presumably this is the dithiol complex of Co^{III}HRP. [d] The sixth ligands of the camphor-bound and camphor-free forms of cobalt-substituted cytochrome $P450_{cam}$ are both indicated here as a H_2O molecule at neutral pH. When pH was raised to 8.5 by addition of 0.1 N KOH, the spectra of both changed drastically, and the species formed are indicated here as the OH^- complexes (ref 23). [e] Taken from Dickinson, L. C.; Chien, J. C. W. *Biochemistry*, **1975**, *14*, 3526.

Table II. Electronic Absorption Spectra of Zinc Porphyrins

	Soret		β		α					
complex[a]	nm	$cm^{-1} \times 10^3$	nm	$cm^{-1} \times 10^3$	nm	$cm^{-1} \times 10^3$	$\epsilon_\alpha/\epsilon_\beta$	$\epsilon_\alpha/\epsilon_B$	solvent[b]	ref
Zn((meso)DME)	404	24.8	532	18.8	569	17.6	1.64	0.082	t	*c*
Zn((meso)DME)	405	24.7	532	18.3	569	17.6	1.55	0.116	t	*f*
Zn((meso)DME)	407	24.6	534	18.7	570	17.5	1.11		d	
Zn((meso)DME)(H_2O)	409	24.4	536	18.7	572	17.55			t	*f*
Zn((meso)DME)(18C6)	412	24.3	538	18.6	575	17.4			t	*f*
Zn((meso)DME)(py)	415	24.1	543	18.4	578	17.3	0.79	0.044	t	*f*
Zn((meso)DME)(Im)	417	24.0	545	18.4	580	17.2	0.80		t	*f*
Zn((meso)DME(pip)	417	24.0	544	18.4	579	17.3	0.82	0.045	t	*f*
Zn((meso)DME)(Im^-)	423	23.6	552	18.2	586	17.1	0193	0.048	t	*f*
Zn((meso)DME)(SBu^-)	438	22.8	562	17.8	(595)	(16.8)	0.236	0.023	t	*c*
Zn((proto)DME)	412	24.3	541	18.5	579	17.3			CCl_4	*d*
Zn(proto)(H_2O)	412	24.3	544	18.4	582	17.2	0.97	0.069	buffer	*e*
Zn((proto)DME)	415	24.1	541	18.5	579	17.3			b	*d*
Zn(Hb)	423	23.6	550	18.2	587	17.0	0.78	0.053	buffer	*e*
Zn(proto)(py)	425	23.5	551	18.2	588	17.0	0.81	0.079	Py	*e*
Zn(OEP)	405	24.7	532	18.8	568	17.6			t	*f*
Zn(OEP)(H_2O)	411	24.3	538	18.6	574	17.4	1.83		t	*f*
Zn(OEP)(18C6)	412	24.3	536	18.6	572	17.5	1.06		t	*f*
Zn(OEP)(Im)	415	24.1	543	18.4	578	17.3	0.80		t	*f*
Zn(OEP)(OH^-)	417	24.0	543	18.4	576	17.4			t	*f*
Zn(OEP)(Im^-)	423	23.6	551	18.1	586	17.1	0.73	0.037	t	*f*

[a] Abbreviations see ref 13. With porphyrin type, entries are listed with increasing red shift. [b] Solvent used: t, toluene, b, benzene; d, dioxane; buffer, pH 7, potassium phosphate, 20 mM. [c] Reference 11. [d] Smith, K. M., Ed., "Porphyrins and Metalloporphyrins"; Elsevier Science Publishing: Amsterdam, 1975. [e] Leonard, J. J.; Yonetani, T.; Callis, J. B. *Biochemistry* **1974**, *13*, 1460. [f] This work.

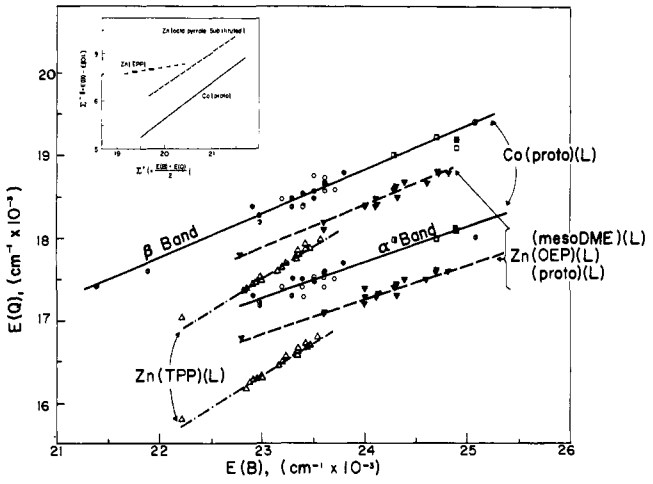

Figure 3. Plot of $E(Q)$ vs. $E(B)$ for ligated forms of cobalt-substituted hemoproteins (Table I), zinc octapyrrole substituted porphyrins (Table II), and Zn(TPP) (ref 11) (see ref 13 for abbreviations used). (○), ●, and ◑ represent ligated Co^{III}(Mb), Co^{III}(HRP), and $Co^{III}(P450_{cam})$, respectively. □, ■, and ◻ represent Co^{II}(MB), Co^{II}(HRP), and Co^{II}-($P450_{cam}$), respectively. ▼ represents ligated Zn(mesoDME) and Zn-(OEP). △ represents ligated Zn(TPP). Lines are best least-squares fits to eq 1, with parameters given in Table III. Inset: Plots of the linear variation of Σ^- with Σ^+ (eq 2), using the parameters (Table III) obtained by least-squares fit of the data in Table II.

state and/or ligation state of the cobalt ion and also that the ratio of α and β band intensity changes in parallel. The Soret and α–β band maxima and relative extinction coefficients of the several cobalt-substituted hemoproteins, namely, myoglobin, horseradish peroxidase, cytochromes P450 and *c*, and their derivatives, are summarized in Table I. Table II gives the band maxima and extinction ratios for a series of Zn((meso)DME)(L) complexes. We first discuss correlations among band positions and then discuss peak intensities.

B–Q Excitation Energies. Figure 3 plots the energies of the α and β band maxima against that of the Soret, or B, band for all of the derivatives of the cobalt-substituted hemoproteins and for the zinc octapyrrole substituted complexes; data for the series of Zn(TPP)(L) complexes reported by Nappa and Valentine[11] are also presented. In the cobalt hemoprotein system, the cluster of points for which the energy of the Soret peak, $E(B)$, is between 23 000 and 23 800 cm^{-1} corresponds to six-coordinate Cobalt(III) hemoproteins with various conventional ligands, while the few cases to the higher side correspond to the five-coordinate cobalt(II) proteins and the substrate-bound form of cobalt(III) cytochrome $P450_{cam}$; the two points given with $E(B) < 22\,500$ cm^{-1} correspond to the cyanide and thiol complexes of the substrate-bound form of cobalt(III) cytochrome $P450_{cam}$, respectively, the only cobalt porphyrin species that exhibits a so-called "hyper" spectrum.[14,23] In these latter two cases only one Q band exists in the visible region; this is common for metalloporphyrin complexes that display "hyper" spectral properties. From the correlations evident in Figure 3 and discussed immediately below, we have provisionally assigned these peaks to the β bands found in the normal metalloporphyrin spectra and *not* to the α bands. Such an assignment is supported when we consider the relationship between transition energies and the ratio of α and β band intensities.

The α band is *nominally* assigned[5,8] to the O–O component of the electgronically forbidden Q band, of excitation energy $E(Q)$; the β band is an envelope of vibronically allowed Q band peaks, with $E(\alpha) - E(\beta)$ corresponding to an average vibrational frequency, $\bar{\nu}$. Linear least-squares fits to the excitation energies are presented in Figure 3. For each of the systems studied, both $E(\alpha) \equiv E(Q)$ and $E(\beta) \equiv E(Q) + \bar{\nu}$ are linearly related to $E(B)$

$$E(\alpha) = E(Q) = s_\alpha E(B) + U_\alpha \quad (1a)$$

$$E(\beta) = E(Q) + \bar{\nu} = s_\beta E(B) + U_\beta \quad (1b)$$

and the fitting parameters are given in Table III. The two slopes

Table III. Least-Squares Parameters Describing the Variation of Optical Transition Energies[a]

complex	slope	intercept, $cm^{-1} \times 10^{-3}$	data
$E(Q) = s_\alpha E(B) + u_\alpha$ (eq 1)			
Co(proto)(L) Zn((meso)DME)(L)	0.43	7.5	*b*
Zn(OEP)(L) Zn(proto)(L)	0.42	7.2	*c*
Zn(TPP)(L)	0.79	−1.8	*d*
$\Sigma^- = t\Sigma^+ + v$ (eq 2)			
Co(proto)(L) Zn((meso)DME)(L)	0.78	−9.9	*b*
Zn(OEP)(L) Zn(proto)(L)	0.77	−9.1	*c*
Zn(TPP)(L)	0.23	2.1	*d*

[a] Plots of data according to eq 1 and of the lines obtained by least-squares fits to eq 1 and 2 are given in Figure 3. [b] Table I; $E(B)$ = Soret in 10^3 cm^{-1} and $E(Q) = \alpha$ energy in 10^3 cm^{-1}. Data from all the complexes are included in the fit except for those of the cobalt(II) cytochrome *c*. [c] Table II. [d] Taken from Table II of ref 11.

are equal within experimental error, $s_\alpha \cong s_\beta$, and thus the frequency $\bar{\nu}$, corresponding to the difference in intercepts for α and β bands, is unaffected by ligation or by changes in $E(B)$. In addition, $\bar{\nu}$ is not significantly different for the three systems: $\bar{\nu} = 1100$–1200 cm^{-1} (see Table III). The slopes of the lines in Figure 3 are essentially the same for the pyrrole-substituted cobalt protoporphyrin and zinc mesoporphyrin series, $s_\alpha \cong 0.5$, whereas for the methine carbon substituted Zn(TPP)(L) series the slope is much greater, $s_\alpha = 0.8$ (table III), although still significantly less than unity.

The observation that $s < 1$ for the three series is of particular interest. It has often before been noted the B and Q bands shift in parallel upon changes in metal or axial ligand, but typically it has been implied that the whole spectrum is red- (or blue-) shifted, which would correspond to a linear relationship between $E(Q)$ and $E(B)$ with $s = 1.0$. No previous systematic observations have noted that $E(B)$ and $E(Q)$ do not in fact shift equally ($s < 1$).

A single linear relationship suffices to correlate optical data for both the six-coordinate Co(III) and five-coordinate Co(II) species, as seen especially in the correlation between β and Soret band frequencies. This can be interpreted as follows: in five-coordinate Co(II) complexes, the additional odd electron is in the $3d_{z^2}$ orbital of the metal atom and is somewhat concentrated in, though not limited to, the sixth coordinate position. As such it can be considered as a "phantom ligand" in analogy to the sixth ligand of a Co(III) complex.

It is useful to recast the correlations between excitation energies in terms of the average energy of the B and Q bands, $\Sigma^+ = (E(B) + E(Q))/2$, and the B–Q energy separation, $\Sigma^- = E(B) - E(Q)$. The individual data sets for the three porphyrin systems each are well represented by the linear equation

$$\Sigma^- = t\Sigma^+ + v \quad (2)$$

with the resultant constants given in Table III and the resulting linear correspondences of Σ^- and Σ^+ displayed in the inset to Figure 3. The utility of eq 2 of course follows from the observation of a linear relation between $E(B)$ and $E(Q)$; the slopes, s in Figure 3 and t in the inset to Figure 3, are related: $t = 2(1 - s)/(1 + s)$.

The recasting has several useful features. First, it emphasizes that the two pyrrole-substituted metalloporphyrin series behave similarly (similar t) even though in one case M = Co and there are two vinyl substituents while in the other M = Zn and all substituents are saturated. In contrast the meso-substituted, TPP, series has M = Zn but behaves quite differently upon ligand variation. Second, it highlights the fact that changes of axial ligand do not merely cause an overall shift of the spectrum, for then horizontal lines, $t = 0$, would obtain. Finally, although the species with "hyper" spectra (the CN^- and thiol complexes of cobalt(III)

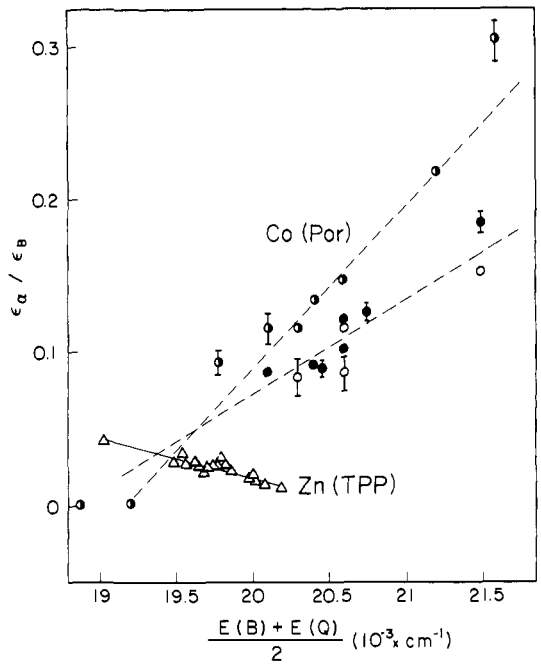

Figure 4. Plot of intensity ratio, $\epsilon_\alpha/\epsilon_\beta$ vs. Σ^+ for cobalt-substituted hemoproteins (Table I) and Zn(TPP) (ref 10). Symbols are as defined in Figure 3. Parameters for linear least-squares fits are given in Table III.

cytochrome P450, the mercaptide complexes of Zn((meso)DME), and Zn(TPP)) fit with the others, their Σ^- values differ somewhat from those predicted from the corelation of Σ^- and Σ^+ for the other species in the same systems. Indeed, least-square fits that satisfy eq 2 were best performed by neglecting data points for the species with hyper spectra were neglected. Such discrepancies are, of course, to be expected. A hyper spectrum in cytochrome P450 to thought to reflect a strong interaction between porphyrin π–π^* configurations and a low-lying charge-transfer transition from a filled p orbital on a mercaptide ligand,[25] in addition to mixing between porphyrin π–π^* configurations. It is not surprising that interaction with the additional charge-transfer configuration weakens the ordinary correlation between excitation energies.

Band Intensities. Figure 4 plots the ratio of intensities for the Q(α) and Q(β) bands, $\epsilon_\alpha/\epsilon_\beta$, vs. the average of the B and Q transition energies, Σ^+. The use of intensities, rather than oscillator strengths, is in keeping with previous work[11,12] and does not obscure any fundamental features. The ratio decreases approximately linearly as Σ^+ increases (blue shift) for the Zn(TPP)(L) complexes as reported by Nappa and Valentine;[11] slopes and intercepts are presented in Table III. Figure 4 also plots $\epsilon^\alpha/\epsilon_\beta$ vs. Σ^+ for the cobalt hemoprotein series. The intensity ratios for the pyrrole-substituted cobalt series increases with Σ^+ (positive slope), in contrast to the Zn(TPP) series, and the dependence on Σ^+ is also stronger (Figure 4). Indeed in the hyperspectra only a single Q peak, the Q(β) band, is observed: $\epsilon_\alpha/\epsilon_\beta \sim 0$. A closer examination of Figure 4 also reveals a distinction between the derivatives of cobalt cytochrome $P450_{cam}$, in which the protein provides a mercaptide anion as the fifth ligand to the central metal ion, and the derivatives of cobalt HRP, Mb, and Hb, in which the protein provides an imidazole from a histidine residue as ligand. These differences probably originate both from a special heme pocket environment and from the unique nature of the anionic and highly polarizable mercaptide as the fifth, endogenous, ligand in $P450_{cam}$.

Discussion

Previous studies have disclosed systematic shifts in metalloporphyrin spectra and changes in extinction coefficient ratios upon variation of metal and/or axial ligand.[4,9–12] The trends observed for the Co and Zn pyrrole-substituted porphyrins clearly are consistent with and support the earlier results. However, Figures 3 and 4 show that ligand substitution does not simply produce an overall spectrum shift, but that Σ^- varies with Σ^+, or alternatively that E(Q) shifts less rapidly than E(B). These trends are strongly influenced by the nature of the porphyrin peripheral substituents, but with only slight variations, the individual axial ligands affect the spectra of the different porphyrin in a similar manner, with the following order of increasing red shift and decreasing intensity ratios: "e^-" < H_2O < F^- < O_2^-, Im, NMeIm < OH^- < N_3^- < CN^-.[11] This latter indicates that the same factors affect the electronic spectra in the two types of peripherally substituted porphyrins. We now show that our observations can be readily understood in terms of the four-orbital model, simply by focusing on changes in the energy of the a_{2u} porphyrin π MO upon changes in axial ligation.

As discussed by Gouterman et al.,[4,6,7] the lowest four excited π–π^* configurations of a fourfold symmetric metalloporphyrin lead to two identical 2 × 2 configuration interaction matrices of which one may be written

$$\begin{vmatrix} \Delta_2 - E & C \\ C & \Delta_1 - E \end{vmatrix} = 0$$

where (see Figure 2) the single-configuration energies are $E(a_2e) = \Delta_2$ and $E(a_1e) = \Delta_1$ with average value Σ^+ and difference 2γ:

$$\Delta_1 = \Delta + \delta + D_1 \quad (3a)$$

$$\Delta_2 = \Delta - \delta + D_2 \quad (3b)$$

$$\Sigma^+ = (\Delta_1 + \Delta_2)/2 \quad (3c)$$

$$2\gamma = \Delta_2 - \Delta_1 \quad (3d)$$

Here 2δ and Δ are the difference and average of the one-electron excitation energies, respectively ($2\delta = \epsilon_{a_2} - \epsilon_{a_1}$ and $\Delta = \epsilon_e - (\epsilon_{a_2} + \epsilon_{a_1})/2$), and D_1 and D_2 are the two-electron contributions to the configuration energies. In Figure 2B the a_2e configuration is taken to be higher in energy than a_1e ($\Delta_2 > \Delta_1$). Since MO calculations indicate $\delta > 0$,[4] this is equivalent to assuming $D_2 - D_1 > 2\delta$ or that $\gamma > 0$; the assumption is validated below. The off-diagonal interaction matrix element between the two configurations is represented by C. Resulting excitation energies are

$$E(B) = \Sigma^+ + [\gamma^2 + C^2]^{1/2} \quad (4a)$$

$$E(Q) = \Sigma^+ - [\gamma^2 + C^2]^{1/2} \quad (4b)$$

with average value

$$(E(B) + E(Q))/2 = \Sigma^+ \quad (5)$$

and with the difference between Soret and α–β band excitation energies of

$$\Sigma^- \equiv E(B) - E(Q) = 2[\gamma^2 + C^2]^{1/2} \quad (6)$$

Note that Σ^+, defined as the average single-configuration energy, is indeed equal to the average excitation energy employed above in the discussion of the experimental observations.

In order to describe the relatively small spectral changes induced by, say, variations in axial ligand, we consider, as reference, a metalloporphyrin ligand complex with median observed value of $E(B)_o$ and write its orbital energies as ϵ_i^o, with other energies subscripted (γ_o, etc.). We assume (see introduction[8,11,12]) that a change of axial ligand merely causes only a small shift in the energy of the a_2 orbital $\epsilon_{a_2}{}^0 \rightarrow \epsilon_{a_2}{}^0 + 2\eta$. More elaborate assumptions provide no further insights. By expression of the square root in eq 6 and retention of only terms linear in η, eq 4 becomes

$$E(B) = E(B)_o - [1 + x]\eta \quad (7a)$$

$$E(Q) = E(Q)_o - [1 - x]\eta \quad (7b)$$

where

$$x = \gamma_o/[\gamma_o{}^2 + C^2]^{1/2} \quad (8)$$

(25) Hanson, L. K.; Eaton, W. A.; Sligar, S. G.; Gunsalus, I. C.; Gouterman, M.; Connell, C. R. *J. Am. Chem. Soc.* **1976**, *98*, 2672–2674.

and the subscripts indicate values for the reference system. By elimination of η

$$E(Q) = [(1 - x)/(1 + x)]E(B) + \text{constant} \quad (9)$$

$$\Sigma^- = (2x)\Sigma^+ + \text{constant} \quad (10)$$

Thus, this treatment generates linear relationships in complete agreement with experiment. Comparison of eq 8 and 9 with eq 1 and 2 shows that $s = (1 - x)/(1 + x)$ and $t = 2x$. The experimental results of Table III, $s < 1$, $t > 0$, indicate that $x > 0$. This requires that the configuration a_2e lies above a_1e, which is equivalent to saying $\gamma_o > 0$, as assumed above. Simple inclusion of changes in ϵ_{a_1} or ϵ_{a_2} would not change the form of these equations but would lead to redefinition of some terms.

Considering the definition of x (eq 8), the slopes s and t are controlled by the relative size of γ_o, which measures the departures of the parent excited configurations from exact degeneracy, and of C, which measures the strength of configuration mixing. Using in eq 9 the experimental values s and t for cobalt protoporphyrin and zinc mesoporphyrin, one obtains $x = 0.4$ and $2\gamma_o \sim C \sim 3600$ cm^{-1}, with the numerical estimate for C being that given by Gouterman et al.[6] In contrast, the values for Zn(TPP) give $x = {}^1/_9$ and a very small departure from degeneracy (one-electron energy difference): $2\gamma_o \sim C/20$, in agreement with ref 6. The range of absorption energies induced by ligand variation corresponds to maximal excursions of the a_{2u} orbital energy ($\epsilon_{a_2}{}^0 \rightarrow \epsilon_{a_2}{}^0 + 2\eta_{max}$), with a magnitude of only $|\eta_{max}| \sim 5 \times 10^2$ cm^{-1} for Zn(TPP) and 8×10^2 cm^{-1} for the pyrrole-substituted complexes; this is quite small compared to $(\Sigma^-)^0 \sim 6\text{–}7 \times 10^3$ cm^{-1}, which justifies the linearization of eq 4 that leads to eq 7–10. Of course, the neglect of terms in η^2 and higher in eq 7, and of any variations in two-electron terms, means that the present results are most useful as qualitative indicators of the relative sizes of the terms involved. Nevertheless, it seems safe to conclude that the differences in spectral properties of the meso- and protoporphyrin systems on one hand and Zn(TPP) on the other reflect the closer approach to a degeneracy of excited configurations in the latter case.

The trends in intensity ratios for the pyrrole-substituted complexes can be rationalized by this simple model. An increase in Σ^+ is caused by an increase in the energy difference between the two parent configurations (2γ). This reduces configuration mixing (for constant C) and as such would be correlated with an increase in $\epsilon_\alpha/\epsilon_B$ and $\epsilon_\alpha/\epsilon_{Soret}$, as observed.[6] This trend also provides an argument for assigning the Q-band of the hyperspectra as the β band.

The intensities for Zn(TPP) cannot be rationalized by this model, for $\epsilon_\alpha/\epsilon_\beta$ decreases as Σ^+ increase (Figure 4). No simple inclusion of possible variations in ϵ_{a_1} which is consistent with the experimental results, $s < 1$ ($t > 0$), can alter this. Rather, for TPP we have concluded that the highest filled levels are more nearly degenerate than those for the other systems, and the inclusion of other effects, such as changes in two-electrons terms, or intrinsic differences between the transition dipoles (a_1e) and (a_2e), probably is required.

Acknowledgment. This work was supported by a grant from the National Institutes of Health (HL 13531). We thank Dr. M. A. Stanford for help in obtaining some of the optical spectra and an anonymous referee for suggesting the possible importance of inequality between the transition dipoles.